

The transverse mode coupling instability and broadband impedance model of the CERN SPS

T.P.R.Linnecar and E.N.Shaposhnikova *
CERN, CH-1211 Geneva 23

Abstract

The intensity of leptons accelerated in the CERN SPS is limited by a vertical transverse instability. The results of measurements of the thresholds for this transverse instability are compared with theoretical predictions for different broadband impedance models of the SPS. The threshold intensities found for the transverse instability and the position of the losses in the cycle enable the parameters of the broadband resonant impedance to be specified.

1 INTRODUCTION

The fast transverse single bunch instability was first observed in PETRA, [1]. Similar effects were seen in several other machines. The phenomenon was explained, [2], by the coupling of head-tail modes, their natural frequencies shifting with increasing beam current due to the interaction with the machine impedance. It was predicted, [3]-[6], that this instability would occur with the lepton beams in the SPS. Fast losses were indeed observed during the first injection tests in 1987. Both analytical estimations and simulation results, [7] -[8], implied that the threshold of the transverse instability should increase during the cycle so that the maximum intensity per bunch that could be transferred to LEP would be defined by the limitations in the SPS at injection, 3.5GeV. However the first tests indicated that a transverse instability leading to strong losses occurred during acceleration at about 12GeV.

Previous papers [4] - [10] used broadband resonator models of the SPS having a transverse shunt impedance Z_t in the range (18 - 47.7)M Ω /m with quality factor $Q=1$, and $Z_t = 102$ M Ω /m with $Q=6$. Resonant frequency f_{res} varied little: (1.3-1.35)GHz. In principle an infinite number of impedance models can fit measurements at fixed conditions. Below by considering the variation of threshold intensity with bunch parameters, we shall try to specify the model more precisely.

Beam parameters change significantly during the cycle in the SPS. At low energy the radiation losses are very small and the long bunches behave like protons. Later on, the radiation becomes more and more important until at top energy this process defines the bunch parameters.

In normal operation during 1993 each lepton cycle in the SPS accelerated 4 electron or positron bunches from 3.5GeV to 20GeV. Chromaticity was positive in both planes ($\sim +0.2$) and the tunes $\nu_x = 0.61$, $\nu_y = 0.58$. Without controlled emittance increase the intensity was limited

by losses in the middle of the cycle. This "high energy" instability is restricted both in time (\sim from 170ms till 270ms after injection, or from 6GeV to 13GeV) and in intensity (from 1.4×10^{10} to 1.9×10^{10}). At injection a bunch of length $\sigma_z = 30$ cm and energy spread $\sigma_E/E = 10^{-3}$ is stable up to 2.1×10^{10} . Above this intensity the bunch suffers first from the transverse mode coupling (TMC) instability and then, above 3.5×10^{10} , from the longitudinal microwave instability. The microwave instability has not been observed at higher energies.

2 INSTABILITY THRESHOLD

The threshold intensity for the TMC instability (zero chromaticity) can be approximated [4] as

$$N_{th} \sim \frac{E_s \nu_s}{e^2 \beta_z Z_t f_{res}} F(\sigma_t f_{res}, Q), \quad (1)$$

where ν_s is the synchrotron tune, β_z is the beta function. The function $F(\sigma_t f_{res}, Q)$ can be calculated numerically. The dependence of the threshold on the bunch length $\sigma_t = \sigma_z/c$, f_{res} and Q is given by the relative positioning in the frequency domain of the machine impedance and bunch spectrum functions. The spectrum for short bunches samples the whole impedance function, whether high or low Q , whereas longer bunches are affected more strongly by the resistive part of the impedance of the lower Q model. So the measurements of thresholds for long and short bunches can give information about the Q of the model. The resonant frequency can possibly be defined in a region where the dependence of function F on $(\sigma_t f_{res})$ is strongly nonlinear. This is true for short bunches with $\sigma_z \sim \sigma_{z0} = c/(2\pi f_{res})$.

To calculate the threshold we used the code MOSES, [11], which searches for solutions of Sacherer's integral equation obtained after expansion of the perturbed distribution function in both azimuthal (modes m), and radial (modes k) coordinates in longitudinal phase space. The appearance of an imaginary part in the solutions for the coherent frequencies with increasing intensity gives the threshold. This occurs when the adjacent mode frequencies, shifted from their unperturbed values, merge together. For the beam with Gaussian distribution the position of the maximum of the spectrum function with modes m and k is $f_{max} = p f_{rev} = (|m| + 2k)^{1/2} c/\sigma_z$. At fixed f_{max} , amplitudes are larger for the spectrum functions with lower azimuthal modes m but higher radial modes k . Hence we cannot ignore the contribution of higher radial modes at least up to $k \sim |m|/2$ if the coupling of mode

*on leave of absence from INR of RAS, Moscow

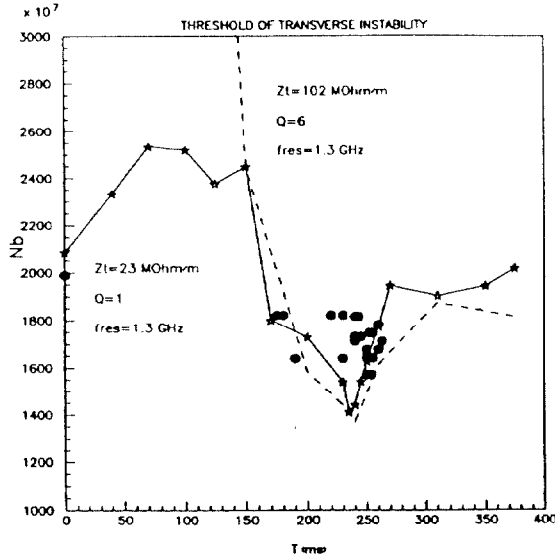


Figure 1: Measurements of beam losses (filled circles) and calculated thresholds for $Q=1$ (solid line) and $Q=6$ (dashed line) models.

m is important, [12]. The number of relevant radial modes k increases with increasing bunch length. Note that results can be very different when only a small number of higher radial modes is included in the calculations.

3 TMC INSTABILITY AT HIGH ENERGIES

The “high energy” instability, (6-13)GeV, is seen as a sharp loss of beam intensity. The losses coincide with strong vertical signals in the 1GHz range with growth rates typically less than a few ms, see [12]. We recorded the loss time and intensity just before the loss. The results of the measurements are shown in Fig.1. Bunches with intensities $(1.9 - 2.1) \times 10^{10}$ suffered losses around 100ms for reasons other than the TMC instability.

To calculate the threshold we need to know the synchrotron frequency and the bunch length at the moment of beam loss. The bunch length can be either measured or calculated. However to use a profile measurement implies that the loss point is known in advance. A technique providing the continuous bunch length (CBL) is very sensitive to calibration errors in the region of instability, where the bunches are short. Hence to know the bunch length we are obliged to use calculation together with measurements.

The SPS cycle uses 100MHz, 200MHz and 352MHz RF systems. We calculated the bunch parameters for a given emittance matched to the bucket in the multiharmonic RF system, taking into account radiation damping and quantum excitation. The calculated bunch length and measurements given by both the CBL measurement (dashed line) taken from the photo and profile measurements (circles) are shown in Fig.2. There is good agreement from 100ms to 240ms. Before 100ms the bunch length is ill-defined due

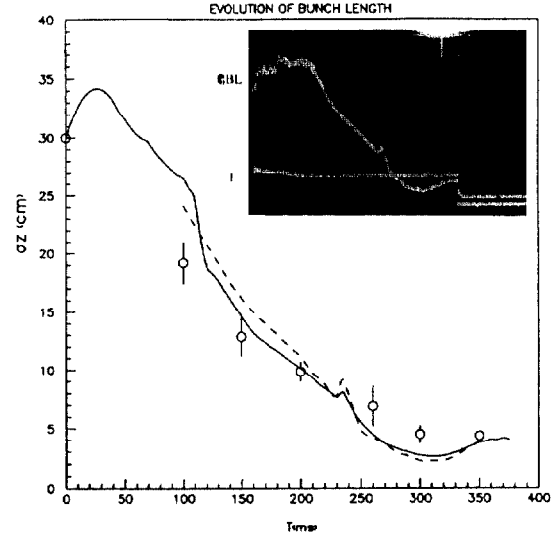


Figure 2: Calculated and measured bunch length evolution. Photo of CBL measurement together with intensity signal (I). Time scale 50 ms/div.

to injection and mismatch errors. The bunch length used in the threshold calculation is the solid line in Fig.2. The synchrotron tune ν_s was also calculated along the cycle.

As a first step for the definition of the impedance model we fixed the resonant frequency at 1.3GHz as suggested before and considered the effect of a variation in Z_t and Q on the threshold intensity.

In Fig.1 we see the TMC threshold calculated by MOSES for the two impedance models, $Q=1$ and $Q=6$, scaled using Z_t to give a good fit around the observed results. For these models this implies $Q=1$, $Z_t = 23\text{M}\Omega/\text{m}$ or $Q=6$, $Z_t = 102\text{M}\Omega/\text{m}$. The first value was found in [9]. The $Q=6$ model was suggested in [10] and used in [7] to explain measurements of instability at injection for 16cm bunches. The calculated thresholds for both models go through a minimum at $\sim 240\text{ms}$ and the experimental points cluster in this dip. Nevertheless only the low Q model is able to explain a maximum intensity observed as well as an earliest time. For the $Q=1$ model as the intensity increases the loss point will move back to 150ms and then jump to injection. Higher intensities are lost at injection. For $Q=2$, and the shunt impedance defined by high energy measurements, a higher threshold is predicted at injection than that observed.

Taking $Q=1$ we now consider varying the resonant frequency. In Fig.3 the thresholds for $f_{res} = 1.5\text{GHz}$, 1.7GHz and 2GHz are shown and can be compared with the results for 1.3GHz, see Fig.1. Thresholds for long bunches, where $F(\sigma_t f_{res}) \sim \sigma_t f_{res}$, are insensitive to the choice of resonant frequency which is not the case for short bunches. As f_{res} increases the dip centred at 235ms decreases in amplitude while another appears at 320ms, and for $f_{res} \sim 2\text{GHz}$ losses should occur at this time in the cycle. For $f_{res} = 1.7\text{GHz}$ we have two dips separated by a small barrier.

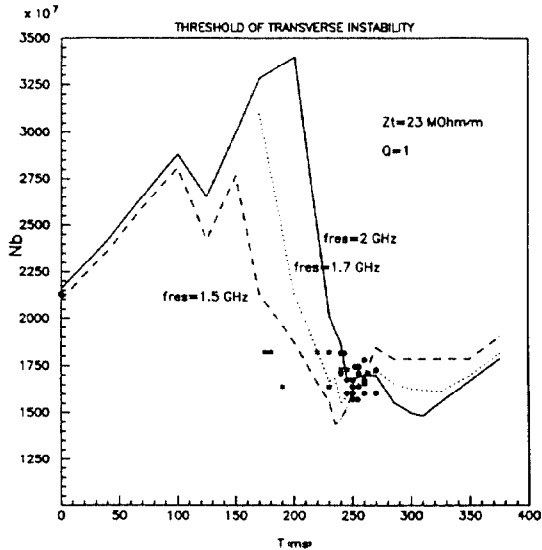


Figure 3: TMC threshold for $f_{res} = 1.5\text{GHz}$ (dashed line), 1.7GHz (dotted line) and 2GHz (solid line) together with measurements (filled circles and crosses).

With the dispersion in bunch length observed during the measurements, if $f_{res} > 1.6\text{GHz}$ we would expect losses in the second dip which were never observed. For $f_{res} \sim 1.5\text{GHz}$, the barrier is re-established. If f_{res} is decreased further it is difficult to explain the narrow region of losses observed. From all the measurements we conclude that f_{res} lies in the range $(1.3-1.6)\text{GHz}$.

4 INSTABILITIES AT INJECTION

The measurements of TMC instability at injection are given in Fig.4, where beam intensity is plotted against bunch length. The parameters of the beam injected into the SPS are well defined due to the fast damping times on the flat top in the injector - CPS. We worked with a single injected bunch captured in a 100MHz bucket.

In general instabilities were present in both planes but their signatures make it possible to disentangle them. Longitudinal instabilities lead to emittance increase but rarely loss, whereas step losses occur with the TMC instability, usually after several revolution periods.

The threshold is not sensitive to resonant frequency for the range of bunch lengths available at injection but is much more affected by changes in Q . Using MOSES the dependence of the threshold on bunch length for impedance models with $f_{res} = 1.3\text{GHz}$ and with different values of Q was found (see Fig.4). These models, as defined by the high energy measurements, all fit well at short bunch lengths but can be distinguished as expected by their behaviour at long bunch lengths. The $Q=1$ model gives the best fit.

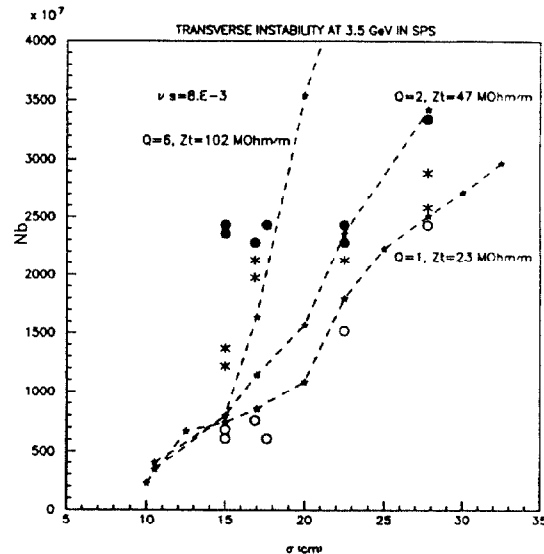


Figure 4: TMC threshold measurements at injection showing the cases of strong (filled circles) and weak (crosses) instability and no instability (empty circles). Calculated thresholds for $f_{res} = 1.3\text{GHz}$ and different Q .

5 CONCLUSIONS

Recent experimental data on the TMC instability seen in the SPS both at high and low energies can be explained using an impedance model defined by a broadband resonator centred at a frequency f_{res} between $(1.3-1.6)\text{GHz}$, with quality factor Q close to 1, and $Z_t \simeq (23 \pm 3)\text{M}\Omega/\text{m}$. The fact that we have losses for short and long bunch regimes allows the determination of Z_t and Q whereas the time of the losses gives f_{res} .

6 ACKNOWLEDGEMENTS

We thank the following people for their help. Y.H.Chin supplied a new, fast version of MOSES. Injection experiments relied on the expertise of J-P.Riinaud. D.Boussard and B.Zotter made helpful comments and suggestions.

7 REFERENCES

- [1] PETRA-Project Group, IEEE-Trans., N26, p.2970, 1979.
- [2] R.D.Kohaupt, report DESY 80-22, 1980.
- [3] J.Gareyte, CERN LEP Note 356, 1982.
- [4] B.Zotter, CERN LEP Note 418, 1982.
- [5] G.Besnier, D.Brandt, B.Zotter, CERN LEP-TH/84-11.
- [6] Y.H.Chin, CERN SPS/86-2 (DI-MST).
- [7] D.Brandt, CERN SPS/AMS/Note/88-7, /88-15.
- [8] D.Brandt et al., CERN SPS/89-6 (AMS).
- [9] D.Brandt, J.Gareyte, CERN SPS/88-17 (AMS).
- [10] L.Vos, CERN SPS/86-21 (MS).
- [11] Y.H.Chin, CERN/LEP-TH/88-05.
- [12] T.Linnecar, E.Shaposhnikova, CERN/SL/93-43 (RFS).